



RESEARCH LETTER

10.1002/2015GL064340

Key Points:

- Lacustrine authigenic mineral formation in relation to climate is examined
- The thresholds for the formation of different minerals are 600, 400, and 350 mm
- Carbonates and evaporites can help in quantitative paleoclimate reconstruction

Supporting Information:

- Figures S1–S5 and Table S1 caption
- Table S1

Correspondence to:

W. Jiang,
wjjiang@mail.iggcas.ac.cn

Citation:

Gu, N., W. Jiang, L. Wang, E. Zhang, S. Yang, and S. Xiong (2015), Rainfall thresholds for the precipitation of carbonate and evaporite minerals in modern lakes in northern China, *Geophys. Res. Lett.*, *42*, 5895–5901, doi:10.1002/2015GL064340.

Received 26 APR 2015

Accepted 7 JUL 2015

Accepted article online 14 JUL 2015

Published online 29 JUL 2015

Rainfall thresholds for the precipitation of carbonate and evaporite minerals in modern lakes in northern China

Ning Gu^{1,2}, Wenying Jiang¹, Luo Wang¹, Enlou Zhang³, Shiling Yang¹, and Shangfa Xiong¹

¹Key Laboratory of Cenozoic Geology and Environment, Institute of Geology and Geophysics, Chinese Academy of Sciences, Beijing, China, ²College of Earth Science, University of Chinese Academy of Sciences, Beijing, China, ³Nanjing Institute of Geography and Limnology, Chinese Academy of Sciences, Nanjing, China

Abstract Authigenic carbonate and evaporite minerals in lake sediments are widely used to qualitatively reconstruct climate. However, uncertainties still remain about their quantitative relationship to climate. Here we investigate 86 modern lakes in northern China to examine the relationships between mineral formation, lake water chemistry, and climate. The results show that from east to west, with increasing salinity and ionic concentration, calcite, dolomite, and evaporite minerals (gypsum and halite) occur in sequence. Their eastern boundaries approximate modern isohyets, and we define for the first time rainfall thresholds of 600 mm, 400 mm, and 350 mm for the formation of calcite, dolomite, and evaporite minerals, respectively. Since the 400 mm and 600 mm isohyets also coincide with vegetation boundaries, our findings enable a new approach for the quantitative reconstruction of paleoprecipitation and paleovegetation based on mineral analysis.

1. Introduction

The precipitation of lacustrine carbonate and evaporite minerals is determined by factors such as the salinity and ionic concentration of the lake water [Eugster and Hardie, 1978; Sonnenfeld and Perthuisot, 1989]. In lake systems, as salinity increases, calcite precipitates first, followed by aragonite and dolomite, and finally sulfates and chlorides [Müller et al., 1972; Nesbitt, 1974; Eugster and Hardie, 1978; Eugster, 1980]. This precipitation sequence is considered to be indicative of increasing aridity, with increasing aridity causing sulfates and chlorides to precipitate rather than carbonates [Eugster and Hardie, 1978; Sonnenfeld and Perthuisot, 1989; Li et al., 1997; Trichet et al., 2001]. However, the hydrochemical and climatic thresholds for the formation of these minerals under natural conditions remain unclear.

The numerous continental lakes in northern China (Figure 1) allow the assessment of the thresholds of lake water chemistry and climatic factors in controlling the precipitation of different lacustrine minerals. First, a steep climate gradient is observed in the region, with mean annual rainfall and temperature decreasing from over 1000 mm and 9°C in the east to 100 mm and 0°C in the west (Figure 1a). Second, the bedrock of the lakes is mainly composed of igneous and metamorphic rocks (mainly granite, basalt, andesite, breccia, and slate) [Ma et al., 2002] (Figure 1c), which to a great extent precludes the presence of detrital carbonate in the lake sediments.

In this study, mineral compositions and water chemistry from a total of 86 lakes (Figure 1c) were investigated and compared with climatic parameters (temperature, rainfall, and aridity), with the objective of exploring the quantitative relationships between water chemistry, climate, and the precipitation of calcite, dolomite, and evaporite minerals in natural lakes in northern China.

2. Materials and Methods

The investigated area (110°E to 130°E, 40°N to 50°N) (Figure 1b) is located in the northern marginal zone of the East Asian monsoon. In winter, the influence of the Siberian-Mongolian High leads to a cold and dry climate, while in summer the southeast monsoon transports heat and moisture inland from the oceans. Surface sediment samples (0 to 0.5–1 cm) from 86 lakes were obtained (Table S1 in the supporting information). Lake water samples were collected from 0.5 to 1 m depth using polyethylene bottles, and pH and conductivity were measured in the field using a HANNA HI 9024 pH meter and a HI 8733 N ATC

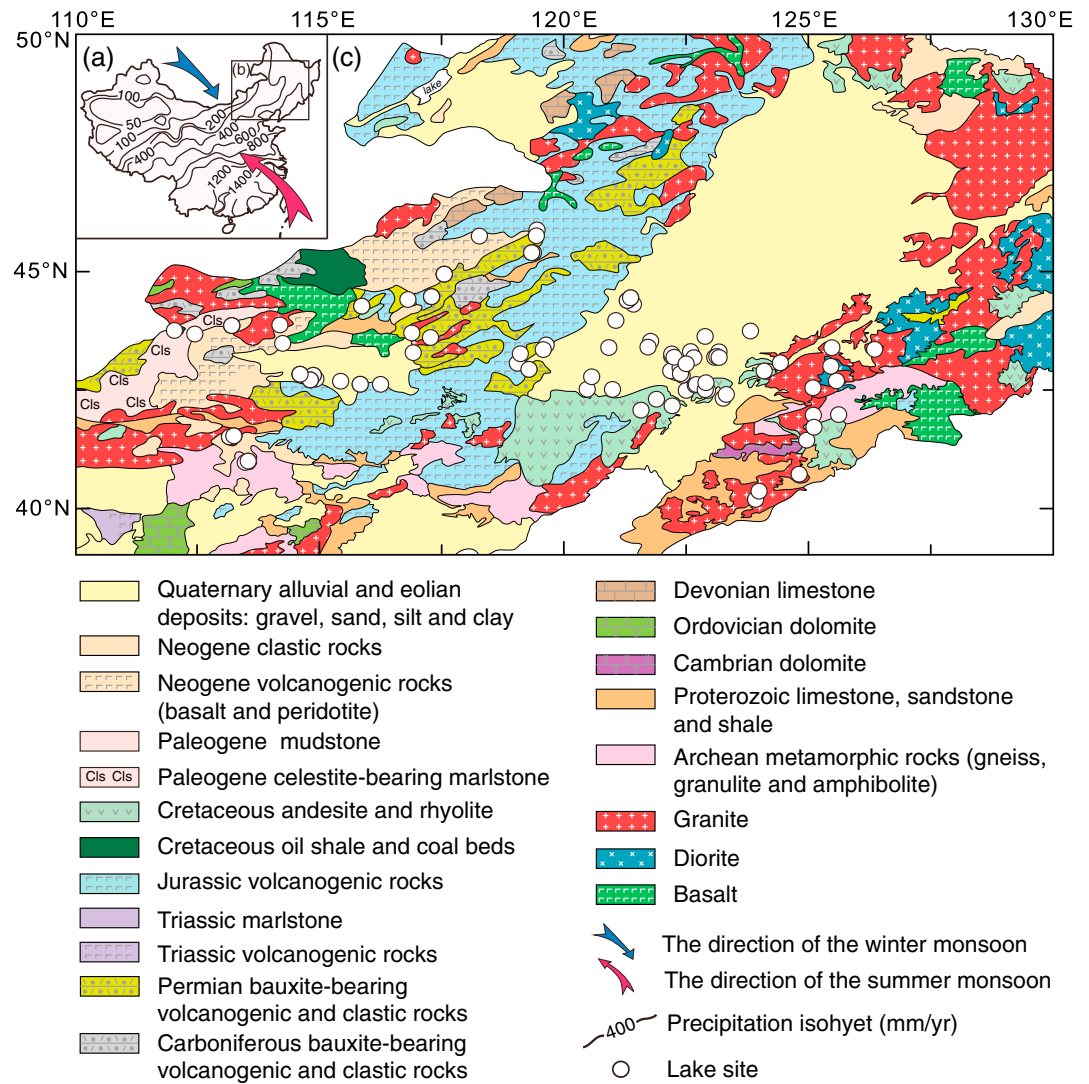


Figure 1. (a) Distribution of mean annual precipitation (mm) in China (data provided by the National Meteorological Information Center of China). (b) Location of the study region. (c) Geological map of the study area (modified from the 1:5,000,000 geological map of China [Commission for the Compilation of the Geological Map of China, 1990]). The blue and red arrows indicate the direction of the winter and summer monsoon, respectively.

multirange conductivity meter, respectively. All sediment samples were freeze dried. Mineral composition and morphology were analyzed using X-ray diffraction (XRD) and scanning electron microscopy (SEM) with an accompanying energy-dispersive analytical facility. Water chemistry analyses were conducted in the State Key Laboratory of Lake Science and Environment, Nanjing Institute of Geography and Limnology, Chinese Academy of Sciences. All water samples were filtered prior to water chemistry analyses. Cation (Mg^{2+} , Ca^{2+} , Na^+ , and K^+) concentrations were determined by inductively coupled plasma-atomic emission spectrometry and anion concentrations (SO_4^{2-} and Cl^-) by ion chromatography (Ics 2000). CO_3^{2-} and HCO_3^- concentrations were measured using a Skalar continuous flow analyzer.

3. Results

The XRD results show that the mineralogical composition of the surface sediments is characterized mainly by quartz, feldspar, carbonate (aragonite, calcite, and dolomite), and evaporite (gypsum and halite) minerals (Figure S1). Eight categories of carbonate and evaporite mineral assemblages were found in the surface sediments: (1) no carbonate or evaporite minerals (Figure S1a, 16 lakes); (2) calcite (Figure S1b, 53 lakes);

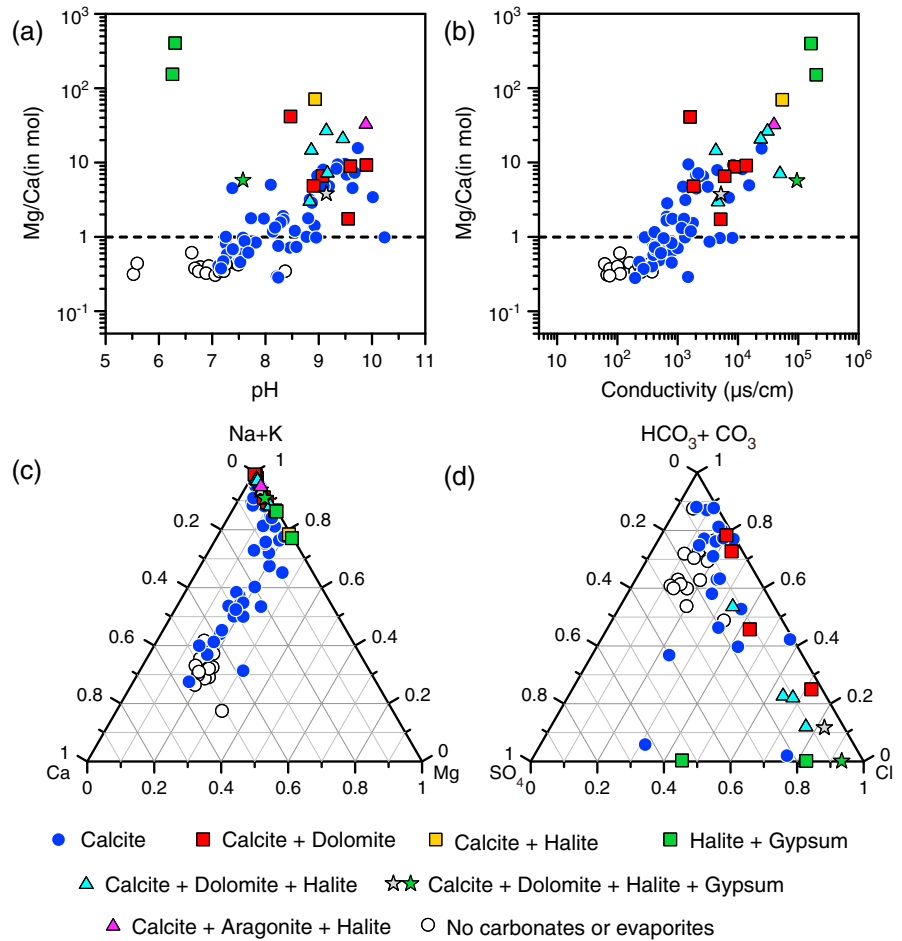


Figure 2. Mg/Ca ratio plotted against (a) pH and (b) conductivity. (c and d) Trilinear plots of the major cations and major anions. Compositions are in mol %. The 86 lakes are divided into eight categories as shown in the legend. Note that (i) the conductivity and pH of the lake water increase from lakes without any carbonate and evaporite minerals, to lakes with calcite, and finally to lakes with dolomite and evaporites; (ii) HCO_3^- , CO_3^{2-} , and Ca^{2+} are high in lakes where calcite precipitates; and (iii) Na^+ , K^+ , and Cl^- are high in lakes containing evaporite minerals.

(3) calcite and dolomite (Figure S1c, 6 lakes); (4) aragonite, calcite, and halite (Figure S1d, 1 lake); (5) calcite and halite (Figure S1e, 1 lake); (6) calcite, dolomite, and halite (Figure S1f, 5 lakes); (7) calcite, dolomite, halite, and gypsum (Figure S1g, 2 lakes); and (8) halite and gypsum (Figure S1h, 2 lakes).

SEM observations of bulk samples reveal that the calcite occurs in the form of clumpy (Figures S2a and S2b) or rhombohedral-blocky (Figures S2c–S2f) grains (5–15 μm). Dolomite spheroids (~1 μm) are attached to the surfaces of other minerals (Figures S3a and S3b) or are aggregated into clusters (Figure S3c). Gypsum occurs either as lenticular crystals (2–10 μm long) (Figure S4a) or in tabular form (~60 μm long) (Figures S4b and S4c). Cubic halite grains have a well-crystallized morphology (10–70 μm) (Figure S5).

Both the conductivity and pH of the lake water increase from lakes without any carbonate and evaporite minerals, to lakes with calcite, and finally to lakes with dolomite and evaporites (Figures 2a and 2b). The lowest values of pH and conductivity for the occurrence of calcite, dolomite, and evaporite minerals are 7.1 and 202 $\mu\text{s/cm}$, 8.4 and 1640 $\mu\text{s/cm}$, and 8.8 and 4380 $\mu\text{s/cm}$, respectively (Table 1). It should be noted that the pH values of the three northwesternmost lakes (Figure 1c) are inconsistent with this trend. These lakes all contain evaporites (gypsum and halite), but the pH values of the lake water are as low as 6.3–7.6 (Figure 2a, two green squares and a green star), which is caused by the very high concentrations of sulfate ion in the lake water [Beamish, 1976] (Figure 4f) due to the weathering of celestite in the bedrock (Figure 1c).

Table 1. Lake Water Chemistry Parameters Required for the Formation of Calcite, Dolomite, Halite, and Gypsum in Northern China

Mineral	PANN ^a (mm)	pH Values	Conductivity (μs)	Na (mmol/L)	K (mmol/L)	Na + K (mmol/L)	Mg (mmol/L)	Ca (mmol/L)	Mg/Ca (in mol)	Cl (mmol/L)	SO ₄ (mmol/L)	HCO ₃ (mmol/L)	CO ₃ (mmol/L)	HCO ₃ + CO ₃ (mmol/L)	NO ₃ (mmol/L)	Number of Lakes
Calcite	600	7.1–7.5	200–500	0.4–2	0.05–0.2	0.4–2	0.1–1	0.2–1	0.2–1	0.1–0.6	0.1–0.3	0.5–2	0.4–3	0.9–5	0.01–0.02	68
Dolomite	350–400	8.4–9.0	1,600–2,000	19–40	0.2–1.5	19–40	1.5–2	0.14–0.3	1.7–5	3.0–5.0	0.2–1.5	6.0–8.0	6.0–8.0	12.0–16.0	0.001–0.03	13
Halite	300–350	8.8–9.4	4,000–20,000	40.0	0.3–2	40–50	0.6–2	0.2–4	3.0–8	14–30	2.0–5.0	1.0–3	0.6–3	1.6–6	0.001–0.02	11
Gypsum	300–350	9.1	5,310	49.7	0.5	50.3	2.5	0.7	3.8	39.3	2.8	2.8	2.8	5.6	0.020	4

^aPANN: the maximum annual precipitation (mm) allowed for the formation of calcite, dolomite, etc. in lakes.

Lakes where calcite precipitates are richer in HCO₃⁻, CO₃²⁻, and Ca²⁺ than other ions, while lakes containing evaporite minerals have higher abundances of Na⁺, K⁺, and Cl⁻ (Figures 2c and 2d). The lowest Mg/Ca (in mol) ratios for lakes in which calcite, dolomite, and evaporite minerals form are 0.2, 1.7, and 3.0, respectively (Table 1).

4. Discussion

The bedrock of the study area is composed of magmatic and metamorphic rocks (mainly granite, basalt, andesite, breccia, and slate), and no limestone or dolostone occurs in the lake catchments [Ma et al., 2002]. In addition, calcite and dolomite grains are all <20 μm in size under SEM. Calcite appears as rhombohedral or blocky grains, and dolomite appears as spheroids or as aggregates of spheroids, resembling in morphology those precipitated in laboratory or natural environments [De Deckker and Last, 1988; Vasconcelos et al., 1995; Vasconcelos and McKenzie, 1997; Filippi et al., 1998; Wright, 1999; Gontharet et al., 2007; Jiang and Liu, 2007; Jiang et al., 2010; Baioumy et al., 2011]. These lines of evidence all suggest an authigenic origin of the calcite and dolomite.

Our investigation reveals a good correlation between Mg/Ca ratios and salinities: higher Mg/Ca ratio corresponds to higher salinity, as indicated by higher conductivity (Figure 2b). The Mg/Ca ratio is considered an important factor controlling the formation of carbonate and evaporite minerals in a lake environment [Müller et al., 1972], but the threshold value remains controversial. For the precipitation of dolomite, it has been suggested that the Mg/Ca ratio should be >5 [Folk and Land, 1975], >2 [Müller et al., 1972], or >1 [Vasconcelos and McKenzie, 1997; Wright, 1999], or even <1 [Roberts et al., 2004; Kenward et al., 2009]. In our study, the lowest Mg/Ca ratio for dolomite lakes is 1.7, while the ratios for lakes where calcite and evaporite minerals form are 0.2 and 3.0, respectively (Table 1). Therefore, the 0.2, 1.7, and 3.0 values for Mg/Ca ratio are considered to be the respective thresholds for the formation of calcite, dolomite, and evaporite minerals in lakes of the East Asian monsoon region.

Salinity and ionic concentrations in lake water are controlled by bedrock weathering [Eugster and Hardie, 1978; Hem, 1985; Giovanoli et al., 1988] and by climatic conditions [Last, 1992]. Our results demonstrate that the eastern boundaries of the distribution of calcite, dolomite, and evaporite minerals correspond approximately to aridity indexes of 3, 4, and 5, respectively (Figure 3a). This consistency indicates the dominant control of aridity over the bedrock weathering on the water chemistry. In northern China, aridity is related more to annual precipitation (Figure 3c) than to temperature (Figure 3b), as indicated by the similarity of the distribution of the contours for precipitation and aridity (Figures 3a and 3c). Thus, in northern China, precipitation is the main factor controlling the water chemistry and the precipitation of lacustrine authigenic minerals. The easternmost limits of the occurrences of calcite, dolomite, and evaporite minerals coincide with the 600 mm, 400 mm, and 350 mm isohyets, respectively (Figure 3c).

The relationship of pH, salinity, and ion concentrations of the lake water with annual precipitation further confirms the control of precipitation on the lacustrine authigenic mineral precipitation sequence. As the annual precipitation decreases from 1100 mm to 600 mm, although there are no carbonate or evaporite minerals in the lakes (Figure 3c), the conductivity, pH, Ca²⁺, Mg²⁺, Na⁺+K⁺, HCO₃⁻+CO₃²⁻, SO₄²⁻, and Cl⁻ concentrations all increase gradually (Figures 4a–4h). When the annual precipitation continues to decrease from 600 to 400 mm, Ca²⁺ decreases slightly (Figure 4a), while the

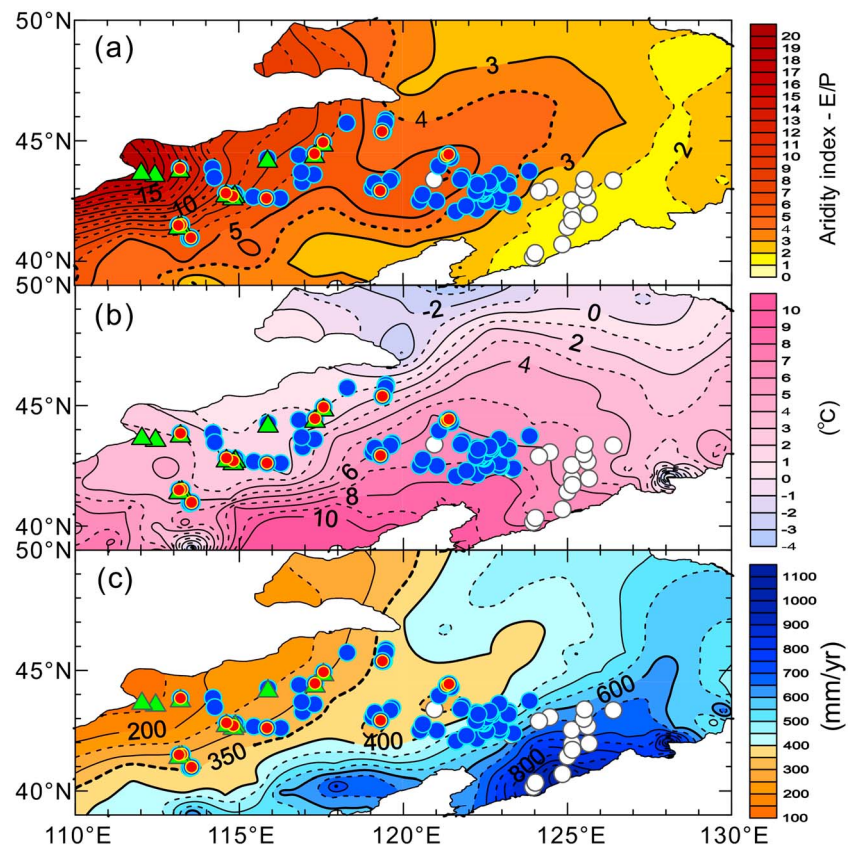


Figure 3. The occurrence of lakes containing calcite (blue dots), dolomite (red dots), or evaporite minerals (green triangles) on isograms of (a) aridity index (E/P), (b) mean annual temperature ($^{\circ}\text{C}$), and (c) annual precipitation (mm). Open circles represent lakes in which carbonate and evaporite minerals are absent. The contour map is compiled using the Surfer Software with 661 data sets from meteorological stations throughout China (data provided by the National Meteorological Information Center of China). Note that the easternmost limits of the occurrences of calcite, dolomite, and evaporite minerals coincide with the 600 mm, 400 mm, and 350 mm isohyets, respectively.

other variables exhibit a generally increasing trend within a relatively large measurement range (Figures 4b–4h). The reason for this is that calcite precipitation removes Ca^{2+} from lake water and affects the residual composition of the water body [Eugster and Hardie, 1978; Evans and Prepas, 1996; Li et al., 1997]. When the annual precipitation decreases to less than 400 mm, conductivity, Mg^{2+} , $\text{Na}^{+} + \text{K}^{+}$, SO_4^{2-} , and Cl^{-} continue to increase, finally resulting in the precipitation of dolomite and evaporites. Thus, the 600 mm and 400 mm isohyets are critical boundaries for the formation of calcite and dolomite, respectively. Interestingly, they also coincide with the modern transitions between forest and forest steppe and between forest steppe and steppe in the study region [Hou, 1988; Editorial Committee of Vegetation Map of China, Chinese Academy of Sciences, 2007].

It is noteworthy that in the area with annual precipitation <600 mm, calcite forms in almost all of the lakes, except for three: one of the three has no carbonate or evaporite minerals in the surface sediments, and the other two exhibit the occurrence of halite and gypsum (Figure 3c). Coincidentally, dolomite and evaporite minerals are not found in several lakes with annual rainfall <400 mm. The reason for this is probably related to microbial metabolism or to the presence of an underground water supply [Jones et al., 1977; Eugster and Hardie, 1978; Wright, 1999; Warthmann et al., 2000; Roberts et al., 2004; Wacey et al., 2007], and the assessment of these possibilities requires further study. For the first time, we have obtained the threshold values of pH, conductivity, major ionic concentrations, Mg/Ca ratio, and rainfall for the formation of calcite, dolomite, and evaporite minerals in natural lakes (Table 1). Therefore, our results provide the basis for a quantitative climatic reconstruction based on lake sediment mineral assemblages in the study region. It should be pointed out that except for the Mg/Ca ratio and rainfall, the values for pH, conductivity, and ionic concentration can be

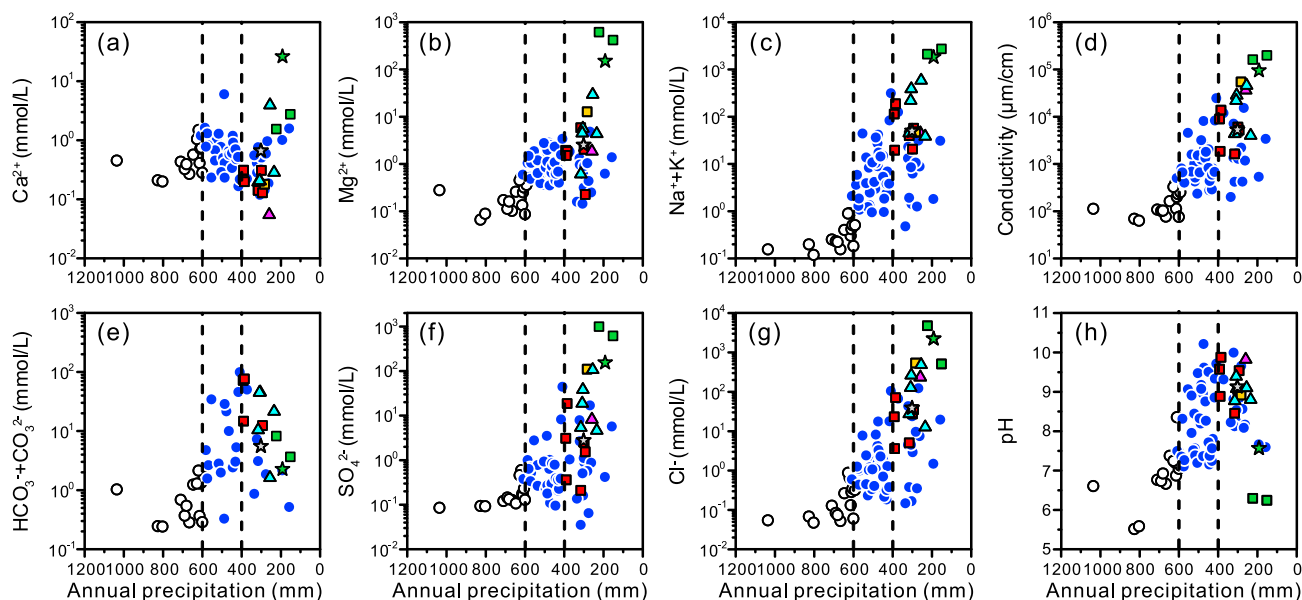


Figure 4. (a–h) Major cations, major anions, pH, and conductivity plotted against annual precipitation for the lake water samples. Symbols are the same as in Figure 3. Precipitation for the 86 lakes was interpolated from 661 data sets from meteorological stations throughout China (data provided by the National Meteorological Information Center of China) using the PPPbase software [Guiot and Goeyry, 1996]. Note that major cations, major anions, pH, and conductivity gradually increase with decreasing annual precipitation. The 600 mm and 400 mm isohyets are critical boundaries for the formation of calcite and dolomite, respectively.

regarded as lower limits since our samples were acquired during the summer monsoon rainy season (Table S1). Finally, we suggest that the study region is unusually well suited to the study of the relationships between the precipitation sequence of carbonates and evaporites and water chemistry and climate.

5. Conclusions

We have conducted mineralogical analyses of the surface sediments of 86 modern inland lakes in the East Asian monsoon region, spanning a range of arid, semiarid, and subhumid environments. The results demonstrate that calcite, dolomite, and evaporite minerals (gypsum and halite) are the main authigenic minerals. From east to west, lake water pH, Mg/Ca ratio, and conductivity increase with decreasing annual precipitation. Comparison of water chemistry and the mineral precipitation sequence demonstrates that Mg/Ca ratios of 0.2, 1.7, and 3.0 are the thresholds for the formation of calcite, dolomite, and evaporite minerals in these lakes, with corresponding pH values of 7.1, 8.4, and 8.8, respectively.

As annual precipitation decreases from east to west, calcite appears first in the surface sediments, followed by dolomite, and finally by evaporite minerals such as gypsum and halite. Comparison of water chemistry and climate factors demonstrates that the lake water chemistry is mainly controlled by aridity, which is causally related to the annual precipitation. The eastern boundaries of the distribution of calcite, dolomite, and evaporite minerals are consistent with the distribution of isohyets, also indicating a strong link between the mineral sequence and rainfall. For the first time we have determined that the easternmost limits of the precipitation of calcite, dolomite, and evaporite minerals coincide with the 600 mm, 400 mm, and 350 mm isohyets, respectively. In addition, the modern 600 mm and 400 mm isohyets are located at the transitions between forest and forest steppe and between forest steppe and steppe in the study region. We conclude that our results provide the basis for a new approach to the quantitative reconstruction of past precipitation and vegetation from geological records.

References

Baioumy, H., H. Kayanne, and R. Tada (2011), Record of Holocene aridification (6000–7000 BP) in Egypt (NE Africa): Authigenic carbonate minerals from laminated sediments in Lake Qarun, *Quat. Int.*, 245(1), 170–177, doi:10.1016/j.quaint.2010.05.021.
 Beamish, R. J. (1976), Acidification of lakes in Canada by acid precipitation and the resulting effects on fishes, *Water Air Soil Pollut.*, 6(2–4), 501–514, doi:10.1007/BF00182888.

Acknowledgments

This study was supported by the National Natural Science Foundation of China (41172157 and 41472318). We thank Yumei Li, Long Han, and Mingqi Luo for their assistance with fieldwork and He Li for his guidance in the XRD analyses. We are grateful to Jan Bloemendal for improving the language and Kim Cobb and an anonymous reviewer for their constructive comments. The XRD data and water chemistry data are provided in a file in the supporting information and will be archived at EarthChem. The meteorological data are available from the National Meteorological Information Center of China.

The Editor thanks Susan Zimmerman for her assistance in evaluating this paper.

- Commission for the Compilation of the Geological Map of China (1990), *Geological Map of China (1: 5 000 000)* [in Chinese], Geological House, Beijing.
- De Deckker, P., and W. M. Last (1988), Modern dolomite deposition in continental, saline lakes, western Victoria, Australia, *Geology*, *16*(1), 29–32, doi:10.1130/0091-7613(1988)016<0029:MDDICS>2.3.CO;2.
- Editorial Committee of Vegetation Map of China, Chinese Academy of Sciences (2007), *Vegetation of China and Its Geographic Pattern—Illustration of the Vegetation Map of the People's Republic of China (1: 1 000 000)* [in Chinese], Geological House, Beijing.
- Eugster, H. P. (1980), Geochemistry of evaporitic lacustrine deposits, *Annu. Rev. Earth Planet. Sci.*, *8*, 35, doi:10.1146/annurev.ea.08.050180.000343.
- Eugster, H. P., and L. A. Hardie (1978), Saline lakes, in *Lakes*, edited by A. Lerman, pp. 237–293, Springer, New York, doi:10.1007/978-1-4757-1152-3_8.
- Evans, J. C., and E. E. Prepas (1996), Potential effects of climate change on ion chemistry and phytoplankton communities in prairie saline lakes, *Limnol. Oceanogr.*, *41*(5), 1063–1076, doi:10.4319/lo.1996.41.5.1063.
- Filippi, M. L., P. Lambert, J. C. Hunziker, and B. Kubler (1998), Monitoring detrital input and resuspension effects on sediment trap material using mineralogy and stable isotopes ($\delta^{18}\text{O}$ and $\delta^{13}\text{C}$): The case of Lake Neuchatel (Switzerland), *Palaeogeogr. Palaeoclimatol. Palaeoecol.*, *140*(1–4), 33–50, doi:10.1016/S0031-0182(98)00040-6.
- Folk, R. L., and L. S. Land (1975), Mg/Ca ratio and salinity: Two controls over crystallization of dolomite, *AAPG Bull.*, *59*(1), 60–68.
- Giovanoli, R., J. L. Schnoor, L. Sigg, W. Stumm, and J. Zobrist (1988), Chemical weathering of crystalline rocks in the catchment area of acidic Ticino lakes, Switzerland, *Clays Clay Miner.*, *36*(6), 521–529, doi:10.1346/CCMN.1988.0360605.
- Gontharet, S., C. Pierre, M. M. Blanc-Valleron, J. M. Rouchy, Y. Fouquet, G. Bayon, J. P. Foucher, J. Woodside, and J. Mascle (2007), Nature and origin of diagenetic carbonate crusts and concretions from mud volcanoes and pockmarks of the Nile deep-sea fan (eastern Mediterranean Sea), *Deep Sea Res., Part II*, *54*(11–13), 1292–1311, doi:10.1016/j.dsr2.2007.04.007.
- Guiot, J., and C. Goeury (1996), PPPBASE, a software for statistical analysis of paleoecological and paleoclimatological data, *Dendrochronologia*, *14*, 295–300.
- Hem, J. D. (1985), Study and interpretation of the chemical characteristics of natural water, Dep. of the Interior, US Geol. Surv.
- Hou, H. (1988), *Physical Geography of China: Phytogeography (II)* [in Chinese], Science Press, Beijing.
- Jiang, W. Y., and T. S. Liu (2007), Timing and spatial distribution of mid-Holocene drying over northern China: Response to a south-eastward retreat of the East Asian monsoon, *J. Geophys. Res.*, *112*, D24111, doi:10.1029/2007JD009050.
- Jiang, W. Y., H. B. Wu, G. Q. Chu, B. Y. Yuan, and Z. T. Guo (2010), Origin of dolomite in Lake Bayanchagan, Inner Mongolia and its palaeoclimatic implications, *Quat. Sci.*, *30*(6), 1116–1120, doi:10.3969/j.issn.1001-7410.2010.06.06.
- Jones, B. F., H. P. Eugster, and S. L. Rettig (1977), Hydrochemistry of the Lake Magadi basin, Kenya, *Geochim. Cosmochim. Acta*, *41*(1), 53–72, doi:10.1016/0016-7037(77)90186-7.
- Kenward, P., R. Goldstein, L. Gonzalez, and J. Roberts (2009), Precipitation of low-temperature dolomite from an anaerobic microbial consortium: The role of methanogenic Archaea, *Geobiology*, *7*(5), 556–565, doi:10.1111/j.1472-4669.2009.00210.x.
- Last, W. M. (1992), Chemical composition of saline and subsaline lakes of the northern Great Plains, western Canada, *Int. J. Salt Lake Res.*, *1*(2), 47–76, doi:10.1007/BF02904362.
- Li, J. R., T. K. Lowenstein, and I. R. Blackburn (1997), Responses of evaporite mineralogy to inflow water sources and climate during the past 100 ky in Death Valley, California, *Geol. Soc. Am. Bull.*, *109*(10), 1361–1371, doi:10.1130/0016-7606(1997)109<1361:ROEMTI>2.3.CO;2.
- Ma, L., X. Qiao, L. Min, B. Fan, X. Ding, and N. Liu (2002), Geological atlas of China: Editorial committee of geological atlas of China.
- Müller, G., G. Irion, and U. Förstner (1972), Formation and diagenesis of inorganic Ca – Mg carbonates in the lacustrine environment, *Naturwissenschaften*, *59*(4), 158–164, doi:10.1007/BF00637354.
- Nesbitt, H. W. (1974), The study of some mineral-aqueous solution interactions, Johns Hopkins Univ.
- Roberts, J. A., P. C. Bennett, L. A. González, G. Macpherson, and K. L. Milliken (2004), Microbial precipitation of dolomite in methanogenic groundwater, *Geology*, *32*(4), 277–280, doi:10.1130/G20246.2.
- Sonnenfeld, P., and J. P. Perthuisot (1989), *Brines and Evaporites*, 126 pp., AGU, Washington, D. C.
- Trichet, J., C. Défarge, J. Tribble, G. Tribble, and F. Sansone (2001), Christmas Island lagoonal lakes, models for the deposition of carbonate–evaporite–organic laminated sediments, *Sediment. Geol.*, *140*(1), 177–189, doi:10.1016/S0037-0738(00)00177-9.
- Vasconcelos, C., and J. A. McKenzie (1997), Microbial mediation of modern dolomite precipitation and diagenesis under anoxic conditions (Lagoa Vermelha, Rio de Janeiro, Brazil), *J. Sediment. Res.*, *67*(3), 378–390, doi:10.1306/D4268577-2B26-11D7-8648000102C1865D.
- Vasconcelos, C., J. A. McKenzie, S. Bernasconi, D. Grujic, and A. J. Tiens (1995), Microbial mediation as a possible mechanism for natural dolomite formation at low temperatures, *Nature*, *377*(6546), 220–222, doi:10.1038/377220a0.
- Wacey, D., D. T. Wright, and A. J. Boyce (2007), A stable isotope study of microbial dolomite formation in the Coorong Region, South Australia, *Chem. Geol.*, *244*(1), 155–174, doi:10.1016/j.chemgeo.2007.06.032.
- Warthmann, R., Y. Van Lith, C. Vasconcelos, J. A. McKenzie, and A. M. Karpoff (2000), Bacterially induced dolomite precipitation in anoxic culture experiments, *Geology*, *28*(12), 1091–1094, doi:10.1130/0091-7613(2000)28<1091:BDPIA>2.0.CO;2.
- Wright, D. T. (1999), The role of sulphate-reducing bacteria and cyanobacteria in dolomite formation in distal ephemeral lakes of the Coorong region, South Australia, *Sediment. Geol.*, *126*(1), 147–157, doi:10.1016/S0037-0738(99)00037-8.